Simulation of the Density-driven Groundwater Flow Using the Meshless Local Petrov-Galerkin Method

Juraj Mužík
University of Zilina, Slovak Republic, muzik@fstav.uniza.sk

ABSTRACT
Density-driven groundwater flow is a complicated nonlinear problem in groundwater hydraulics. The local Petrov-Galerkin method is a promising meshless scheme that is used for solving several difficult problems in different areas. This method applies the weak form of governing equations to the local mesh around every node. The nodes can be randomly distributed in the domain and on the global boundary. Therefore, this method is characterized as meshless. The unknown potentials and concentrations in all of the nodes are approximated by interpolation to obtain a system of linear equations. Solving this system of equations leads to the numerical solution for the main problem. In this paper, a combination of the radial basis function interpolation and the local Petrov-Galerkin method is used to solve groundwater flow problem combined with the transport of pollution, which also influences the density of groundwater..

Keywords: *meshless Local Petrov-Galerkin method, Solute transfer, Density-driven flow, Radial basis functions*

1 INTRODUCTION

Density-driven groundwater flow appears mainly in saltwater intrusion and geothermal processes. Some environmental problems, such as leakage from landfills, can also be influenced by changes in the density and viscosity of groundwater. Modeling density-driven flow problems requires a coupled groundwater flow and transport numerical model. The coupling is realized using the state equations that link density and viscosity variations to pollution concentration or temperature. This coupled problem is nonlinear; therefore, the simulation usually requires large meshes and extensive computational time, even for simulations of testing examples. Because of the high computational costs, most authors have focused on vertical 2D numerical models, although the problems are generally three-dimensional. The typical numerical methods used to solve these problems are based on different formulations of the finite element method (Kolditz et al., 1998; Simpson and Clement, 2003) or the discontinuous Galerkin method (Ackerer and Younes, 2008; Younes et al., 2009). In this paper, we present a meshless numerical method based on the local Petrov-Galerkin method (MLPG) to reduce the large computational requirement. The meshless local Petrov-Galerkin method (MLPG) was introduced by Atluri et al.[5]. This method is characterized as meshless because distributed nodal points that cover the domain are employed. These nodal points can be randomly distributed over the domain. Every node is surrounded by a quadrilateral mesh centered at this point. The unknown variable at this point is then expressed using a weak formulated equations on this local mesh. All of these unknown variables are approximated by interpolation to obtain a system of linear equations. Solving this system of equations leads to the numerical solution. Atluri et al. (2001) used the moving least squares (MLSs) method for the interpolation, but the radial basis functions (RBFs) interpolation has also been used (Sellountos and Sequeira, 2008; Kovarik et al., 2012). Here, the solution of the coupled groundwater flow-mass transfer problem, based on the MLPG is presented.

2 GOVERNING EQUATIONS AND LOCAL WEAK FORMULATION

Density-driven groundwater flow can be written in terms of an equivalent fresh water potential (Ackerer and Younes, 2008)

$$\rho S \frac{\partial h}{\partial t} + \varepsilon \frac{\partial \rho}{\partial x} + \nabla \cdot (\rho \mathbf{q}) = 0 \tag{1}$$

where h is the equivalent fresh water potential, ε is the porosity of the porous medium, and ρ is the density of the solution. $\mathbf{q}$ is the Darcy velocity defined as

$$\mathbf{q} = -\mathbf{K}\left(\nabla h + \frac{\rho - \rho_0}{\rho_0} \nabla \bar{z} \right) \tag{2}$$

where $\mathbf{K}$ is the matrix of hydraulic conductivities and ρ_0 is the initial density of fresh water. To simplify the groundwater flow equation (1), we used the Boussinesq approximation, i.e. density variations are neglected and only the buoyancy term of the Darcy equation depends on the density (Kolditz et al., 1998). The differential equation of 2D groundwater flow with variable density is now expressed as

$$\frac{\partial}{\partial x}\left(K_x \frac{\partial h}{\partial x} \right) + \frac{\partial}{\partial y}\left[K_y \left(\frac{\partial h}{\partial y} + \frac{\rho - \rho_0}{\rho_0} \right) \right] = S \frac{\partial h}{\partial t} \tag{3}$$

where we denote the hydraulic conductivities in x and y directions as K_x and K_y, respectively. The solute mass conservation can be written in terms of the solute concentrations as

$$\varepsilon \frac{\partial C}{\partial t} = \nabla \cdot (\mathbf{D} \cdot \nabla C) - \mathbf{q} \cdot \nabla C \tag{4}$$

where C is the solute concentration and $\mathbf{D}$ is the dispersion tensor. The flow and transport equations are coupled by a state equation linking the density to the solute concentration. For the density, we use a linear model

$$\rho = \rho_0 + (\rho_C - \rho_0)\bar{C} \tag{5}$$

where ρ_c is the density of injected fluid. $\bar{C}$ is the relative concentration defined as

$$\bar{C} = \frac{C}{C_{max}} \tag{6}$$

where C_{max} is the maximum mass concentration. Eq.(3) can be transformed to the following shape

$$\frac{\partial^2 h}{\partial x^2} + \frac{K_y}{K_x}\frac{\partial^2 h}{\partial y^2} = \frac{S}{K_x}\frac{\partial h}{\partial t} - \frac{K_y}{K_x \rho_0}\frac{\partial \rho}{\partial y} \tag{7}$$

To transform (7) to the Poisson equation, we use the following transformation of coordinates

$$\tilde{x} = x \qquad \tilde{y} = y\sqrt{\frac{K_x}{K_y}} \tag{8}$$

and we obtain

$$\frac{\partial^2 h}{\partial \tilde{x}^2} + \frac{\partial^2 h}{\partial \tilde{y}^2} = \frac{S}{K_x}\frac{\partial h}{\partial t} - \frac{1}{\rho_0}\sqrt{\frac{K_y}{K_x}}\frac{\partial \rho}{\partial \tilde{y}} \tag{9}$$

To solve (9) in a two-dimensional domain Ω with a boundary Γ, we apply the weighting residual principle with the Green integration formula (Kovarik, 2000) and we obtain the weak form which will be later discretized using MLPG approach.

3 THE MLPG METHOD AND THE LOCAL WEAK FORMULATION

The meshless Local Petrov-Galerkin method (MLPG) is truly meshless method which requires no elements or global background mesh, for either interpolation or integration purposes. In MLPG the problem domain is represented by a set of arbitrarily distributed nodes (Lin and Atluri, 2001).

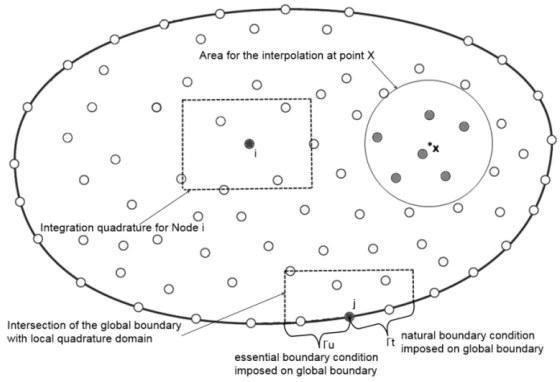

Figure 1 Schematic of local quadrature domain, essential and natural interested boundary.

The weighted residual method is used to create the discrete system equation by integrating the governing equation over local quadrature domains (see. Fig.1). The quadrature domain can be arbitrary in theory, but very simple regularly shaped domain, such as rectangles for 2D problems are often used for ease of implementation.

A generalized local weak form of the Poisson equation (9) defined over local sub-domain Ω_s using backward time difference can be written as

$$\int_{\Omega_s}\left[\frac{\partial^2 h^{n+1}}{\partial\tilde{x}^2}+\frac{\partial^2 h^{n+1}}{\partial\tilde{y}^2}-\frac{S}{K_x}\frac{h^{n+1}}{\Delta t}\right]w d\Omega = \int_{\Omega_s}\left[\frac{h^n}{\Delta t}-\frac{1}{\rho_0}\sqrt{\frac{K_y}{K_x}}\frac{\partial\rho^{n+1}}{\partial\tilde{y}}\right]w d\Omega \quad (10)$$

where index n means time step and w is the test function defined as

$$w(r_i)=\begin{Bmatrix}1-6r_i^2+8r_i^3-3r_i^4;\ r_i\le 1\\ 0\qquad\qquad\qquad ;\ r_i>1\end{Bmatrix}\quad r_i=\frac{\|x-x_i\|}{d_s} \quad (11)$$

where d_s is the size of the local quadrature domain, so it is evident that weighting function value is zero on its boundary. The choice if this test function is motivated by its ability to vanish on the boundary of local quadrature domain. Using the divergence theorem the (10) has changed to

$$\int_{\Omega_s}\frac{\partial h^{n+1}}{\partial\tilde{x}}\frac{\partial w}{\partial\tilde{x}}d\Omega-\int_{\Gamma_{su}}\frac{\partial h^{n+1}}{\partial\tilde{x}}w n_{\tilde{x}}d\Gamma+\int_{\Omega_s}\frac{\partial h^{n+1}}{\partial\tilde{y}}\frac{\partial w}{\partial\tilde{y}}d\Omega- \int_{\Gamma_{su}}\frac{\partial h^{n+1}}{\partial\tilde{y}}w n_{\tilde{y}}d\Gamma+\frac{S}{\Delta t K_x}\int_{\Omega_s}w h^{n+1}d\Omega= \int_{\Gamma_{sq}}\frac{\partial h^{n+1}}{\partial\tilde{x}}w n_{\tilde{x}}d\Gamma+\int_{\Omega_s}h^n w d\Omega-\frac{1}{\rho_0}\sqrt{\frac{K_y}{K_x}}+\int_{\Omega_s}\frac{\partial\rho^{n+1}}{\partial\tilde{y}}d\Omega \quad (12)$$

The values of potential h and density are expressed using the RBF interpolation functions as follow

$$h=\sum_{i=1}^{N}\varphi_i h_i \qquad \rho=\sum_{i=1}^{N}\varphi_i\rho_i \quad (13)$$

where φ is RBF shape function for ith node and N is number of nodes used for interpolation, in this case the Multi-Quadrics Radial Basis function (MQ-RBF), details can be found in (Kovarik et al., 2012).

After substituting (13) into (12) the nodal constants h_i and ρ_i can be moved out of the integral the equation (12) can be expressed as discrete system of linear equations to solve the potential at every node. The mass transfer equations are solved using the same MLPG method and algorithms similar to those used for the potential flow equation. The equations of flow and mass transfer are then coupled by the equation of state, which makes the fluid density a function of the mass solute fraction. The coupling scheme was realized by a sequential-iterative approach using the modified Pickard algorithm according to (Ackerer et al., 2004):

- Step 1: Solve the transfer equations.
- Step 2: Update the fluid density.
- Step 3: Solve the potential flow.
- Step 4: Compute the velocities of flow.
- Step 5: Test the convergence of the process.

This modified scheme converges faster than the classical Pickard algorithm (Ackerer et al., 2004).

4 NUMERICAL EXAMPLE - SIMULATION OF THE HENRY PROBLEM

Unfortunately, we cannot use the usual verification procedure based on exact analytical solutions in this case due to the nonlinear nature of the density-driven problems and we must rely only on comparison with other numerical solutions. Therefore, the MLPG model has been compared with standard Henry saltwater intrusion problem. Numerical example was solved on a workstation equipped with two

Intel I7 4510U CPUs and 16 GB memory. The generalized minimal residual (GMRES) method with simple Jacobi preconditioning was used to solve system of equations (for potentials and concentrations) in every time step and iteration.

Table 1 The parameters of the Henry problem.

S.	Quantity	Value	Unit
ϵ	Porosity	0.35	-
K	Hydraulic conductivity	1.0010×10^{-2}	$m\ s^{-1}$
D_m	Molecular diffusion (Henry solution)	6.6×10^{-6}	$m^2\ s^{-1}$
D_m	Molecular diffusion (Pinder solution)	2.31×10^{-6}	$m^2\ s^{-1}$
q	Discharge of fresh water	6.6×10^{-5}	$m^2\ s^{-1}$
ρ_0	Fresh water density	1000	$kg\ m^{-3}$
ρ_c	Solute density	1025	$kg\ m^{-3}$
S_s	Specific storage	0.0	m^{-1}

The Henry problem is one of the most popular tests used for density driven flow models. This is a 2D problem describing saltwater intrusion into a confined rectangular aquifer that was initially saturated with freshwater. The geometry of the problem is shown in Fig. 2.

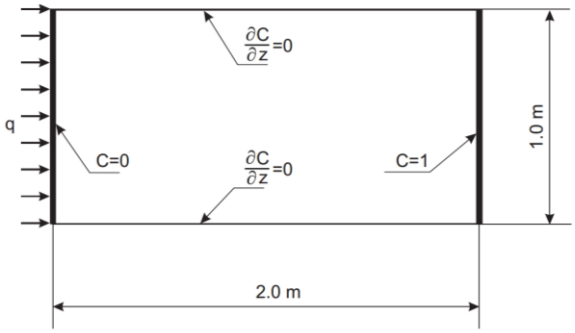

Figure 2 The geometry and boundary conditions of the Henry problem.

The boundary conditions for flow consist of two impermeable parts in the top and bottom of the aquifer. The right vertical part of the boundary is considered the seaside boundary, and a hydrostatic pressure is defined along it. A constant inflow of freshwater into the solved area is assumed along the opposite vertical part of the boundary. Therefore, the boundary conditions for solute transport are quite simple. The maximum concentration $C_{max}=1$ is assigned to the seaside right vertical part of the boundary, and the freshwater condition ($C=0$) is defined along the opposite left vertical part. The zero-flux conditions are used on both horizontal parts of the boundary (Fig. 2). The properties of this problem are listed in Table 1.

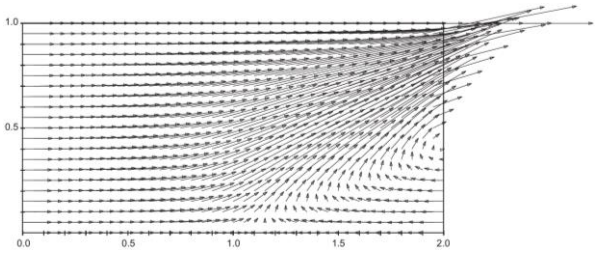

Figure 3 The velocity vectors for the original Henry problem.

In the right bottom part of the rectangular domain (where the density is the highest), the gradient of the hydraulic head is oriented vertically upward, and the gravitational force points vertically downward. These two forces generate a nearly horizontal flow of seawater into the aquifer. The solute density decreases along the bottom part of the boundary as a result of the influence of the freshwater flow from the left-hand side. Finally, the velocity directions are redirected back to the upper right side (Fig. 3). The simulation was performed on 861 regularly distributed nodes (41 horizontally and 21 vertically) (Fig. 4).

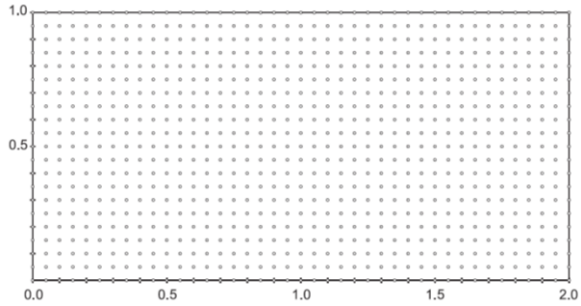

Figure 4 Regular computational network for the solution of the Henry problem.

The initial condition of the problem was an aquifer filled by freshwater. Two different coefficients of molecular diffusion were used for the simulation (Table 1). The first one corresponds to the Henry (1964) solution, and the second one corresponds to the Pinder

solution (1970). The resulting isochlors are presented in Figs. 5 and 6.

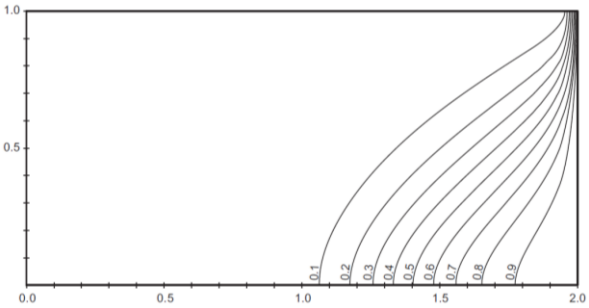

Figure 5 The solute mass concentrations for the original Henry problem.

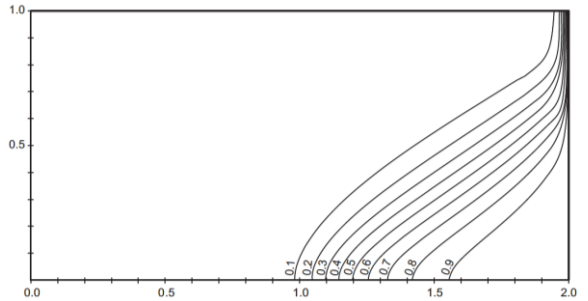

Figure 6 The solute mass concentrations for the Pinder modification of the Henry problem.

The iterative scheme used the modified Pickard algorithm, and the subsequent iterations were employed until the maximum *L2* error in the concentration value for every time step was less than $1x10^{-5}$. For the isochlor *C=0.5*, Fig. 7 compares the simulation results of the original Henry problem with those of other reports (Henry, 1964; Lee and Cheng, 1974; Gotovac et al., 2003; Soto et al., 2007). The results of Voss and Souza's simulation (1987), which used slightly different boundary condition and did not employ the Boussinesq approximation, are also included in this figure. Similarly, Fig.8 compares the isochlor *C=0.5* for the Pinder modification with those of different authors (Pinder and Cooper, 1970; Segol et al., 1975; Gotovac et al., 2003).

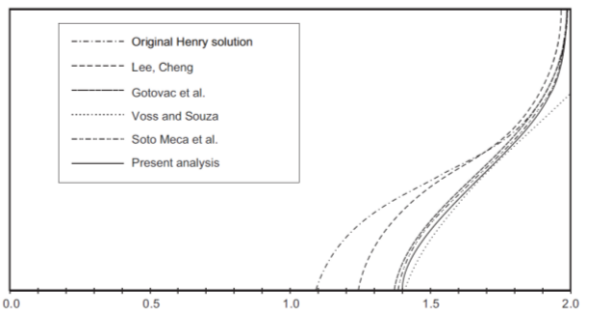

Figure 7 A comparison of the isochlor C=0.5 for the original Henry problem from different authors.

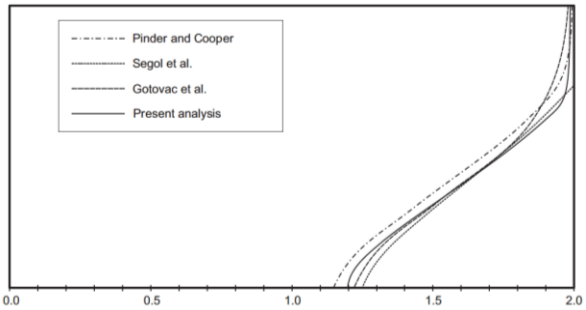

Figure 8 A comparison of the isochlor C=0.5 for the Pinder modification from different authors.

5 CONCLUSIONS

This paper presents a possible use of the MLPG meshless method to model density-driven flow. This method appears to be effective and useful for modeling the density-driven flow. This research is at its initial stages, and a follow-up study should focus on the modification of existing algorithms to enable distributed processing. Choosing suitable tools that allow parallel solving of very large network systems, which usually exist in practical solutions, are needed.

6 REFERENCES

Ackerer P, Younes A, Mancip M (2004). A new coupling algorithm for density-driven flow in porous media. Geophys Res Lett;31:L12506.

Ackerer P, Younes A (2008). Efficient approximations for the simulation of density driven flow in porous media. Adv Water Res;31:15–27.

Divo E, Kassab AJ (2007). An efficient localized radial basis function meshless method for fluid flow and conjugate heat transfer. Trans ASME;129:124–36.

Franke R (1982). Scattered data interpolation: tests of some methods. Math Comput;38:181–99.

Golberg M, Chen C, Bowman H (1999). Some recent results and proposals for the use of radial basis functions in the BEM. Eng Anal Boundary Elem; 23:285–96.

Gotovac H, Andricevic R, Gotovac B, Kozulic V, Vranjes M (2003). An improving collocation method for solving the Henry problem. J Contam Hydrol ;64:129–49.

Hardy RL (1990). Theory and applications of the multiquadrics-biharmonic method (20 years of discovery 1968–1988). Comput Math Appl;19:163–208.

Henry HR (1964). Effects of dispersion on salt encroachment in coastal aquifers, sea water in coastal aquifers. US Geol Surv Supply Pap;1613-C:70–84.

Kansa EJ (1990). Multiquadrics a scattered data approximation scheme with application to computational fluid dynamics. Comput Math Appl;19:127–45.

Kolditz O, Ratke R, Diersch HG, Zielke W (1998). Coupled groundwater flow and transport: 1. Verification of variable density flow and transport models. Adv Water Res;21:27–46.

Kovarik K, Muzik J, Mahmood MS (2012). A meshless solution of two dimensional unsteady flow. Eng Anal Boundary Elem;36:738–43.

Kovarik K (2000). Numerical models of groundwater pollution. Springer-Verlag.

Larsson E, Fornberg B (2003). A numerical study of some radial basis function based solution methods for elliptic PDEs. Comput Math Appl;46:891–902.

Lee CH, Cheng TS (1974). On seawater encroachment in coastal aquifers. Water Resour Res;10:1039–43.

Lin H., Atluri S.N (2001). The Meshless Local Petrov-Galerkin Method for Solving Incompressible Navier-Stokes Equations, Computer Modeling in Engineering & Sciences, pp. 117–142.

Pinder GF, Cooper Jr. HH (1970). A numerical technique for calculating the transient position of the saltwater front. Water Resour Res;6:875–82.

Segol G, Pinder GF, Gray WG (1975). A Galerkin-finite element technique for calculating the transient position of the saltwater front. Water Resour Res;11:343–7.

Sellountos EJ, Sequeira A (2008). An advanced meshless LBIE/RBF method for solving two-dimensional incompressible fluid flows. Comput Mech;41:617–31.

Shu C, Ding H, Yeo KS (2003). Local radial basis function-based differential quadrature method and its application to solve two-dimensional incompressible Navier–Stokes equations. Comput Methods Appl Mech Eng;192:941–54.

Simpson MJ, Clement TP (2003). Theoretical analysis of the worthiness of Henry and Elder problems as benchmarks of density-dependent groundwater flow models. Adv Water Res;26:17–31.

Soto Meca A, Alhama F, Gonzalez Fernandez CF (2007). An efficient model for solving density driven groundwater flow problems based on the network simulation method. J Hydrol;339:39–53.

Voss CI, Souza WR (1987). Variably density flow and solute transport simulation of regional aquifers containing a narrow fresh-water saltwater transition zone. Water Resour Res;23:1851–66.

Younes A, Fahs M, Ahmed S (2009). Solving density driven flow problems with efficient spatial discretizations and higher-order time integration methods.Adv Water Res;32:340–52.